Collisions of low-energy electrons with isopropanol

M. H. F. Bettega
Departamento de Física, Universidade Federal do Paraná, Caixa Postal 19044, 81531-990, Curitiba, Paraná, Brazil

C. Winstead and V. McKoy
A. A. Noyes Laboratory of Chemical Physics, California Institute of Technology, Pasadena, California 91125, USA

A. Jo, A. Gauf, J. Tanner, L. R. Hargreaves, and M. A. Khakoo
Department of Physics, California State University, Fullerton, California 92834, USA
(Received 16 August 2011; published 5 October 2011)

We report measured and calculated cross sections for elastic scattering of low-energy electrons by isopropanol (propan-2-ol). The experimental data were obtained using the relative flow technique with helium as the standard gas and a thin aperture as the collimating target gas source, which permits use of this method without the restrictions imposed by the relative flow pressure conditions on helium and the unknown gas. The differential cross sections were measured at energies of 1.5, 2, 3, 5, 6, 8, 10, 15, 20, and 30 eV and for scattering angles from 10° to 130°. The cross sections were computed over the same energy range employing the Schwinger multichannel method in the static-exchange plus polarization approximation. Agreement between theory and experiment is very good. The present data are compared with previously calculated and measured results for *n*-propanol, the other isomer of C_3H_7OH. Although the integral and momentum transfer cross sections for the isomers are very similar, the differential cross sections show a strong isomeric effect: In contrast to the *f*-wave behavior seen in scattering by *n*-propanol, *d*-wave behavior is observed in the cross sections of isopropanol. These results corroborate our previous observations in electron collisions with isomers of C_4H_9OH.

DOI: 10.1103/PhysRevA.84.042702 PACS number(s): 34.80.Bm, 34.80.Gs

I. INTRODUCTION

Recent studies of electron collisions with methanol (CH_3OH) and ethanol (C_2H_5OH) [1], *n*-propanol (C_3H_7OH) and *n*-butanol (C_4H_9OH) [2], and the other isomers of C_4H_9OH, namely isobutanol, *t*-butanol, and 2-butanol [3], show a broad structure in the elastic integral cross section (ICS) of each molecule around 10 eV. However, the differential cross sections (DCSs) of the straight-chain molecules, namely ethanol, *n*-propanol, and *n*-butanol, show an *f*-wave scattering pattern between 5 to 10 eV, while branched systems such as isobutanol, *t*-butanol, and 2-butanol show a *d*-wave pattern. Similar behavior was also seen in alkanes [4–12]. These results suggest that the DCS of isopropanol (propan-2-ol or isopropyl alcohol), the branched isomer of C_3H_7OH, should also exhibit a *d*-wave pattern. To explore this question, we have carried out a joint experimental and theoretical study of elastic electron collisions with isopropanol. The differential cross sections were measured at incident energies between 1.5 and 30 eV and for scattering angles from 10° to 130° using the relative flow technique with helium as the standard gas and a thin aperture as the collimating target gas source. Calculations using the Schwinger multichannel (SMC) method in the static-exchange plus polarization (SEP) approximation were performed for the same range of energies. The influence of the long-range dipole potential on the cross sections was included in the calculations through Born closure on the scattering amplitude.

The outline of the paper is as follows: In Sec. II, the experimental setup is described, while Sec. III briefly describes the method employed in the calculations. In Sec. IV, the results are presented and discussed. The paper concludes with a brief summary of the present findings.

II. EXPERIMENT

The experimental apparatus has been described in previous articles (e.g., Khakoo *et al.* [13]) so only a brief description will be given here. The apparatus consisted of a spectrometer using crossed target and electron beams, housed in a high-vacuum chamber evacuated to a base pressure of $\sim 2 \times 10^{-7}$ Torr by a single 10-inch diffusion pump. The electron gun and the detector employed double hemispherical energy selectors, with cylindrical lenses used to transport and focus electrons. The spectrometer was baked to about 130 °C by magnetically free biaxial heaters (ARi Industries model BXX06B41-4K). The remnant magnetic field in the collision region was reduced to less than 1 mG by using a double μ-metal shield as well as a single Helmholtz coil that eliminated the vertical component of the Earth's magnetic field. The beam produced by the electron gun could be focused at electron energies down to 1.5 eV, with an energy resolution of 45–50 meV [full width at half maximum (FWHM)]. Typical beam currents were around 20 nA. Over many weeks of the measurements, the spectrometer required minor periodic tuning to maintain the long-term stability of the current, which varied by no more than 10% at any time. The energy of the electron beam was established within an uncertainty of ±20 meV by recording the beam energy required to observe the dip in the He elastic-scattering cross section due to the $2\,^2S$ He^- resonance. The contact potential was found to be 0.664 ± 0.030 eV, determined as the difference between the observed energy of this dip and its established energy of 19.366 eV [14]. Energy-loss spectra of the elastic peak were collected at fixed incident electron energy (E_0) values and electron scattering angles θ by repetitive, multichannel scaling techniques. Scattered electrons entered the analyzer and were

detected by a discrete dynode electron multiplier (Equipe Thermodynamique et Plasmas model AF151). The detection efficiency of the detector remained constant for electron count rates up to 1 MHz, without saturating, while the background count rate was <0.01 Hz. The angular resolution of the electron analyzer was 2° FWHM.

The effusive target gas beam was formed by flowing gas through a thin aperture of 0.3 mm diameter, described previously [15]. This aperture, located 6 mm below the axis of the electron beam, was incorporated into a movable source arrangement [16]. The movable gas source method has been well tested previously [17] and enabled the expedient and accurate determination of background scattering rates. The gas needle, as well as all other metal surfaces exposed to the electron beam, were coated in soot from an acetylene flame to reduce the emission of secondary electrons. The pressures behind the source for isopropanol and helium were about 0.1 and 1.0 Torr, respectively, and the pressure in the experimental chamber was $\sim 1 \times 10^{-6}$ Torr with the gas beam on. The gas beam temperature, determined by the apparatus temperature in the collision region, was about 130 °C; however, in most of the gas-handling copper tubing, the temperature was 65 °C, with the higher temperature only in the last 4 cm of the gas handling system before the gas exited into the collision region. The gas-kinetic molecular diameter of isopropanol was determined, based on the flow rate vs. drive pressure analysis [17], to be 7.36×10^{-8} cm, slightly smaller than that of *n*-propanol (7.49×10^{-8} cm) at a temperature of 74 °C [1].

Elastic scattering measurements were taken at E_0 values of 1.5, 2.0, 3.0, 5.0, 6.0, 8.0, 10.0, 15, 20, and 30 eV for scattering angles ranging from 10° to 130°. Integral elastic and momentum-transfer cross sections (MTCSs) were computed from the measured DCS by extrapolating the DCS to 0° and 180°, using theory as a guide where possible. At energies below 5 eV, the extrapolation to forward angles was guided using the Born-dipole form of the DCS for a dipole moment of 1.66 Debye (D) [18] and a rotational energy loss of 5 meV. Above this energy, the present calculated data were used to guide the extrapolation.

III. THEORY

The cross section calculations were performed with the SMC method implemented for parallel computers. Both the method [19] and implementation [20] have been described in detail elsewhere, so here only those aspects that are relevant to the present study are discussed.

The bound-state and scattering calculations for isopropanol employed the same procedure as was used for *n*-propanol [2]. The geometry of the ground state was optimized within the C_s point group using GAMESS [21] at the level of second-order Møller-Plesset perturbation theory (MP2) in the 6-31G(*d*) basis set. The resulting structure is shown in Fig. 1 (generated using MacMolPlt [22]), which also shows *n*-propanol for comparison. Although the minimum-energy conformation of gas-phase isopropanol appears to be a somewhat different C_1 structure [23], based on previous results for *n*-propanol and *n*-butanol [2], it is expected that carrying out the calculations in the C_s group does not affect the cross sections significantly.

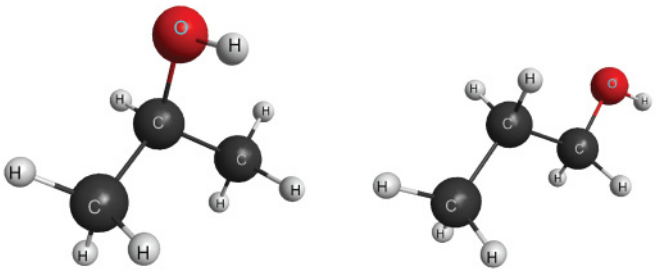

FIG. 1. (Color online) Geometrical structure of C_3H_7OH isomers. Left, isopropanol; right, *n*-propanol.

The ground-state electronic wave function at the optimized geometry was described at the Hartree-Fock level with the DZV++G(2*d*,1*p*) basis set. Scattering calculations were carried out in the SEP approximation. In the SMC method, polarization effects are taken into account through single (virtual) excitations promoting an electron from an occupied (hole) orbital of the Hartree-Fock ground state to an unoccupied (particle) orbital. These *N*-particle configurations are then antisymmetrized with one-particle (scattering) orbitals to construct the $(N + 1)$-particle basis set. Modified virtual orbitals (MVOs) [24] were employed to represent the particle and the scattering orbitals. The MVOs were generated from a cationic Fock operator with charge +6. Singlet-coupled excitations from the 10 highest hole orbitals into the 20 lowest particle (MVOs) were included, while all MVOs were used as scattering orbitals. This procedure resulted in 10 346 double configuration state functions (CSFs) for A' symmetry and 10 207 CSFs for A'', for a total of 20 553 CSFs.

The permanent dipole moment of isopropanol has been measured to be 1.66 D [18] and 1.58 D [25], similar to that of *n*-propanol (1.55 D). The present calculation yields a larger value of 1.86 D (see Table I). The long-range character of the dipole potential was accounted for in the scattering amplitude by the standard Born closure procedure [1]. The SMC amplitude was retained up to an ℓ_{SMC} ranging from 1 or 2 at low energy, to between 3 and 5 at intermediate energies, and up to 12 at higher energies. Table I shows a comparison between the symmetry group, the computed and the experimental dipole moments, and the number of CSFs used in the *n*-propanol and isopropanol calculations.

IV. RESULTS AND DISCUSSION

The measured DCS and corresponding ICS and MTCS data are given in Table II, along with the experimental uncertainties.

TABLE I. Symmetry groups used in our calculations, computed and experimental dipole moments μ (Debye), and the number of CSFs per symmetry (A' and A'') for the SEP calculations, for the two C_3H_7OH isomers.

Molecule	Group	μ	μ_{expt}	A'	A''
n-propanol	C_s	1.69	1.55[b]	10423	10130
isopropanol	C_s	1.86	1.66[a]; 1.58[b]	10346	10207

[a]Reference [18].
[b]Reference [25].

TABLE II. Measured differential cross sections (10^{-16} cm^2/sr) for elastic electron scattering by isopropanol. The second column at each energy lists the error estimate. The entries in italic are extrapolated values used in computing the integral elastic σ_I and momentum-transfer σ_{MT} cross sections, which are listed, along with their error estimates, at the foot of the columns. The notation [n] signifies 10^n.

θ (deg)	1.5 eV		2 eV		3 eV		5 eV		6 eV		8 eV		10 eV		15 eV		20 eV		30 eV	
0	*6.12[5]*		*8.17[5]*		*1.23[6]*		*3.75[5]*		*2.53[5]*		*1.34[5]*		*8.93[4]*		*5.95[4]*		*8.93[4]*		*4.17[4]*	
1	*4.71[3]*		*3.54[3]*		*2.37[3]*		*3.75[3]*		*2.54[3]*		*1.36[3]*		*9.20[2]*		*6.25[2]*		*9.61[2]*		*4.72[2]*	
3	*527*		*395*		*264*		*416*		*289*		*168*		*127*		*96.1*		*167*		*101*	
5	*190*		*142*		*94.9*		*149*		*110*		*72.2*		*62.5*		*53.1*		*101*		*68.9*	
8	*74.2*		*55.7*		*37.1*		*58.5*		*47.8*		*38.9*		*39.3*		*36.9*		*74.8*		*53.6*	
10	*47.6*		*35.7*		*23.8*		*37.9*		32.2	7.34	31.0	7.98	28.3	5.76	28.8	2.32	60.8	2.98	47.0	4.04
15	14.3	2.55	*15.9*		14.1	1.16	20.5	2.08	20.8	3.09	22.3	2.32	17.8	1.93	19.5	1.41	30.0	1.86	21.0	1.26
20	7.49	0.99	8.24	0.55	6.68	0.62	13.9	1.15	13.4	1.69	14.0	1.22	12.3	0.80	9.97	0.67	11.8	0.61	10.1	0.53
30	5.55	0.66	3.40	0.25	3.75	0.20	6.68	0.48	6.74	0.35	5.39	0.57	5.17	0.26	4.63	0.42	4.20	0.21	2.49	0.12
40	2.40	0.25	2.57	0.15	2.68	0.21	3.70	0.21	3.33	0.21	2.59	0.16	2.60	0.16	2.83	0.17	2.35	0.10	1.97	0.13
50	2.29	0.20	2.04	0.13	2.71	0.12	3.25	0.24	2.67	0.16	2.11	0.16	2.13	0.11	2.24	0.11	2.29	0.10	1.45	0.08
70	2.35	0.16	2.23	0.12	2.56	0.21	2.52	0.17	1.88	0.17	1.27	0.12	1.45	0.09	1.29	0.08	0.97	0.05	0.63	0.03
90	2.12	0.12	1.71	0.13	1.79	0.13	2.01	0.13	1.76	0.18	1.55	0.13	1.51	0.11	1.02	0.06	0.73	0.04	0.38	0.02
110	1.76	0.13	1.20	0.06	1.33	0.05	1.97	0.09	1.58	0.16	1.37	0.13	1.26	0.07	0.98	0.04	0.79	0.04	0.60	0.04
130	1.87	0.24	0.90	0.05	1.22	0.07	1.97	0.09	1.54	0.15	1.40	0.12	1.54	0.10	1.35	0.06	0.99	0.06	0.81	0.05
140	*1.85*		*0.88*		*1.20*		*2.01*		*1.63*		*2.02*		*2.54*		*1.70*		*1.17*		*1.00*	
150	*1.70*		*0.89*		*1.15*		*2.43*		*2.31*		*3.10*		*3.47*		*2.04*		*1.43*		*1.20*	
160	*1.50*		*0.87*		*1.10*		*3.14*		*3.22*		*4.39*		*4.57*		*2.49*		*1.73*		*1.44*	
170	*1.30*		*0.83*		*1.05*		*3.70*		*3.96*		*5.46*		*5.51*		*2.90*		*2.03*		*1.72*	
180	*1.10*		*0.81*		*1.05*		*3.88*		*4.22*		*5.87*		*5.89*		*3.06*		*2.15*		*1.85*	
σ_I	63.1	30.9	48.7	24.3	43.2	14.4	63.9	24.3	52.0	15.4	42.7	11.5	40.0	9.44	33.0	5.36	37.8	6.76	26.4	3.87
σ_{MT}	24.6	2.66	17.0	1.05	19.9	1.35	29.3	2.92	25.1	4.14	25.1	6.79	26.2	7.16	18.8	2.79	14.4	1.77	10.8	1.58

Figure 2 compares the measured and computed DCS, which agree very well except at 20 and 30 eV, where the calculated results are larger. At these higher energies, there are many open channels, including ionization, but the present single-channel calculation does not allow flux to escape into them from the elastic channel. As expected, the long-range dipole potential dominates the low-angle scattering, leading to a sharp increase in the DCS there. Both the calculated and the measured DCS exhibit clear d-wave behavior at 6, 8, and 10 eV. For comparison, Fig. 3 contrasts the DCS of isopropanol

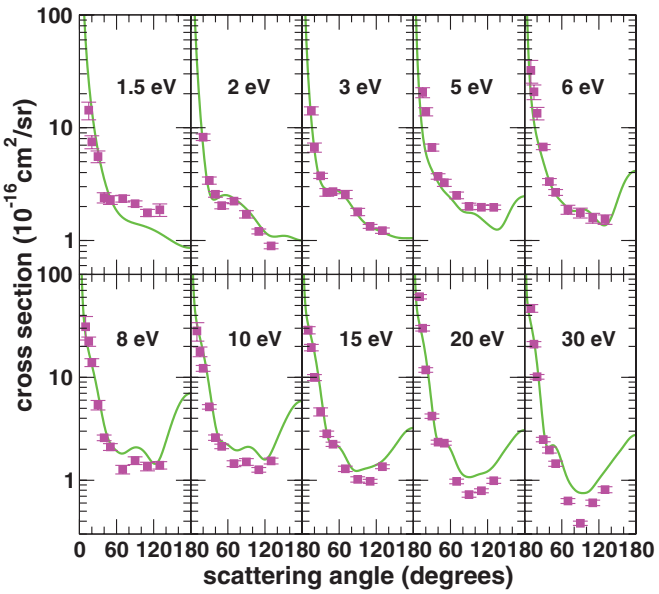

FIG. 2. (Color online) Differential cross sections for isopropanol. Solid (green) line, present computed results; squares (magenta), present experimental data.

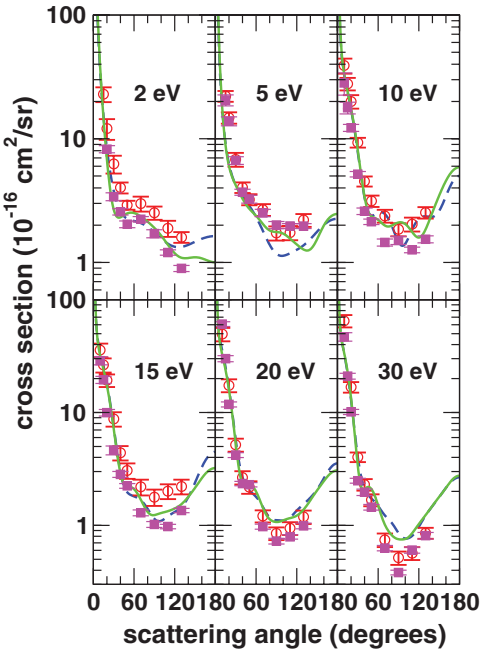

FIG. 3. (Color online) Differential cross sections for the C_3H_7OH isomers at selected energies. Solid (green) line, present computed results for isopropanol; dashed (blue) line, n-propanol; squares (magenta), present experimental data for isopropanol; open circles (red), experimental data for n-propanol. The results for n-propanol were taken from Ref. [2].

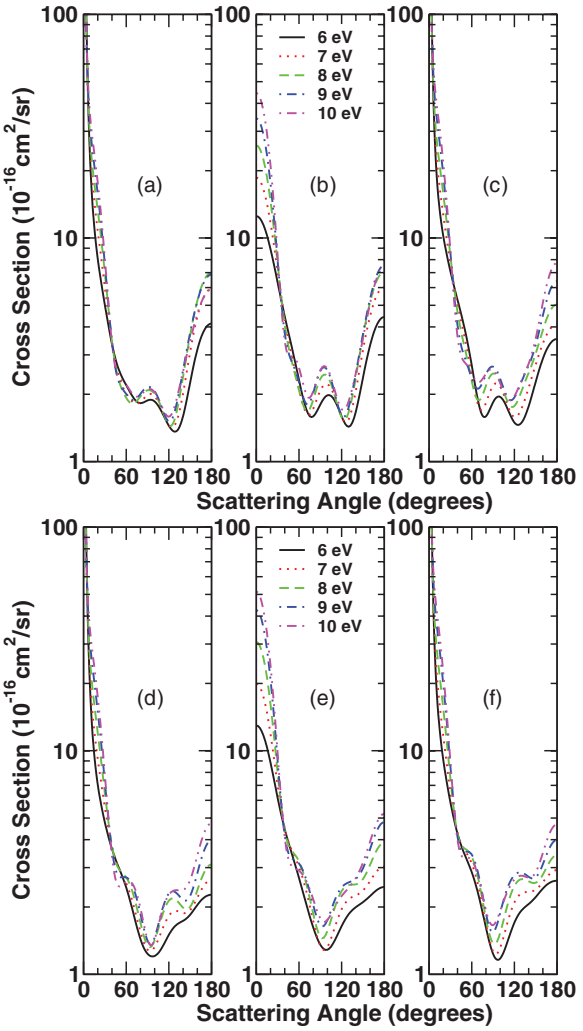

FIG. 4. (Color online) Calculated differential cross sections for (a) isopropanol, (b) isobutane, (c) isobutanol, (d) *n*-propanol, (e) *n*-butane, and (f) *n*-butanol at 6, 7, 8, 9, and 10 eV. The results for isobutane and *n*-butane are from Ref. [12], those for isobutanol, from Ref. [3], and those for *n*-propanol and *n*-butanol from Ref. [2]. See text for discussion.

with previous results [2] for *n*-propanol, which displays a distinct *f*-wave pattern at intermediate angles. These isomeric differences are further exhibited in Fig. 4, which compares calculated DCS at 6, 7, 8, 9, and 10 eV for isopropanol, *n*-propanol, isobutanol, *n*-butanol, isobutane, and *n*-butane [2,3,12]. This extended comparison shows that the branched-chain molecules isopropanol, isobutane, and isobutanol have a dominant *d*-wave scattering pattern, while their straight-chain isomers *n*-propanol, *n*-butane, and *n*-butanol have a dominant *f*-wave pattern. Clearly, the arrangement of the atoms within the molecule, including the location of the hydroxyl group, affects the leading partial-wave contributions to the DCSs. We note that 2-butanol, not shown in Fig. 4, also displays the *d*-wave pattern of a branched system [3].

Figure 5 shows the present calculated and measured ICS for isopropanol in comparison with our previous results for *n*-propanol [2]. The cross sections of the two isomers are similar at all energies. Agreement between the calculated and

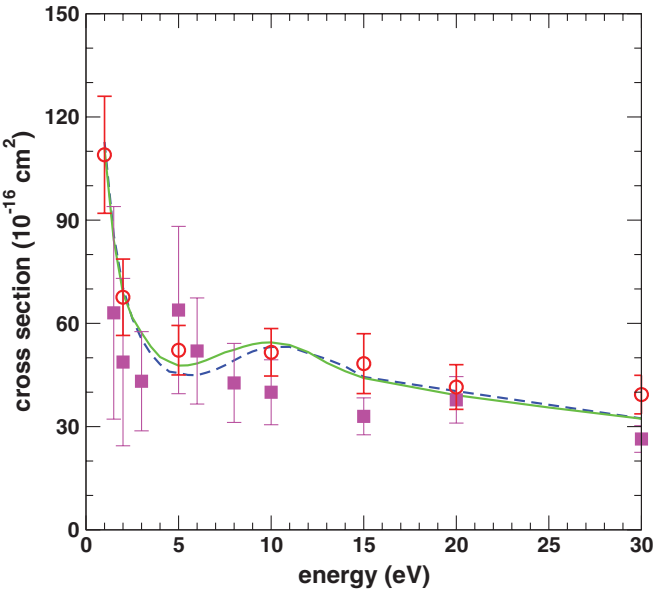

FIG. 5. (Color online) Integral cross sections for the C_3H_7OH isomers. Solid (green) line, present computed results for isopropanol; dashed (blue) line, *n*-propanol; squares (magenta), present experimental data for isopropanol; open circles (red), experimental data for *n*-propanol. The results for *n*-propanol were taken from Ref. [2].

experimental ICS for isopropanol is good, though not as good as for *n*-propanol [2], with the calculated cross sections lying inside the error bars at all energies. The main feature in the ICS is a broad maximum at around 10 eV. Similar structures are present in the ICS of methanol, ethanol, *n*-propanol, and the isomers of butanol [1–3], but also in the ICS of alkanes

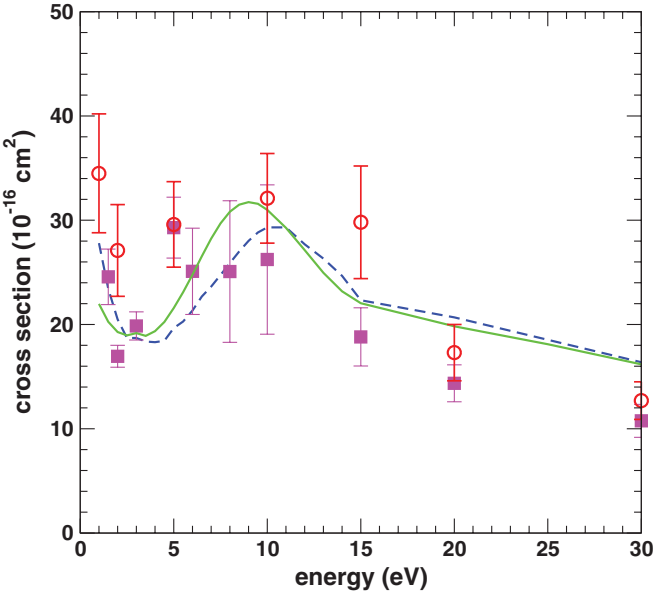

FIG. 6. (Color online) Momentum transfer cross sections for the C_3H_7OH isomers. Solid (green) line, present computed results for isopropanol; dashed (blue) line, *n*-propanol; squares (magenta), present experimental data for isopropanol; open circles (red), experimental data for *n*-propanol. The results for *n*-propanol were taken from Ref. [2].

and alkenes, suggesting an association with short-lived C-H and/or C-C σ^* resonances rather than a specific connection to the alcohols. The MTCS for isopropanol is shown in Fig. 6, together with previous theoretical and experimental data for *n*-propanol [2]. A broad maximum near 10 eV is again evident and the MTCSs of the two isomers are again similar.

V. SUMMARY

Measured and computed elastic differential, integral, and momentum-transfer cross sections have been presented for electron collisions with isopropanol at energies from 1.5 to 30 eV. Good agreement is found between the experimental and theoretical results. While the integral and momentum-transfer cross sections of isopropanol and *n*-propanol are similar in magnitude and both show a broad maximum near 10 eV, the differential cross sections are distinct, with isopropanol showing predominantly *d*-wave and *n*-propanol predominantly *f*-wave character in the ∼6–10 eV range. Similar behavior was observed for the isomers of C_4H_9OH and has also been seen in scattering by linear and branched alkanes [3].

Because the *d*- or *f*-wave scattering behavior is observed in gases at or above room temperature, which may contain more than one conformer, and because calculations that assume nonoptimal conformers having C_s symmetry agree well with the measurements, the scattering pattern appears to depend only on the general arrangement of the atoms in the molecule (i.e., straight vs. branched chains) and not on conformational details such as the orientation of the hydrogens within CH_3 or OH groups. It is also remarkable that (with the exception of methanol) each alcohol should have the same scattering behavior as the alkane obtained by replacing the polar OH group with a nonpolar CH_3 group. Whether the same holds true for the NH_2 and F groups that are also isoelectronic with OH remains to be determined, as existing electron scattering data for aminoalkanes and monofluoroalkanes are quite limited.

ACKNOWLEDGMENTS

This work was funded through a collaborative program by the US National Science Foundation under Grant Nos. PHY 0653452 and PHY 0653396 and by the Brazilian Conselho Nacional de Desenvolvimento Científico e Tecnológico (CNPq) under Project No. 490415-2007–5. M.H.F.B. also acknowledges support from the Paraná state agency Fundação Araucária and from FINEP (under Project No. CT-Infra), as well as computational support from Professor Carlos M. de Carvalho at DFis–UFPR and at LCPAD–UFPR. Work by V.M. and C.W. was also supported by the Chemical Sciences, Geosciences, and Biosciences Division, Office of Basic Energy Sciences, Office of Science, US Department of Energy. The authors acknowledge the use of the Jet Propulsion Laboratory's Supercomputing and Visualization Facility, where the present calculations were performed.

[1] M. A. Khakoo, J. Blumer, K. Keane, C. Campbell, H. Silva, M. C. A. Lopes, C. Winstead, V. McKoy, R. F. da Costa, L. G. Ferreira, M. A. P. Lima, and M. H. F. Bettega, Phys. Rev. A **77**, 042705 (2008).

[2] M. A. Khakoo, J. Muse, H. Silva, M. C. A. Lopes, C. Winstead, V. McKoy, E. M. de Oliveira, R. F. da Costa, M. T. doN.Varella, M. H. F. Bettega, and M. A. P. Lima, Phys. Rev. A **78**, 062714 (2008).

[3] M. H. F. Bettega, C. Winstead, and V. McKoy, Phys. Rev. A **82**, 062709 (2010).

[4] D. Matsunaga, M. Kubo, and H. Tanaka, in *Proceedings of the 12thInternational Conference on the Physics of Electronic and Atomic Collisions,* edited by S. Datz (North-Holland, Amsterdam, 1981), p. 358.

[5] P. J. Curry, W. R. Newell, and A. C. H. Smith, J. Phys. B **18**, 2303 (1985).

[6] H. Tanaka, L. Boesten, D. Matsunaga, and T. Kudo, J. Phys. B **21**, 1255 (1988).

[7] W. Sun, C. W. McCurdy, and B. H. Lengsfield III, J. Chem. Phys. **97**, 5480 (1992).

[8] L. Boesten, M. A. Dillon, H. Tanaka, M. Kimura, and H. Sato, J. Phys. B **27**, 1845 (1994).

[9] M. H. F. Bettega, R. F. da Costa, and M. A. P. Lima, Phys. Rev. A **77**, 052706 (2008).

[10] M. H. F. Bettega, R. F. da Costa, and M. A. P. Lima, Braz. J. Phys. **39**, 68 (2009).

[11] A. R. Lopes, M. H. F. Bettega, M. A. P. Lima, and L. G. Ferreira, J. Phys. B **37**, 997 (2004).

[12] M. H. F. Bettega, M. A. P. Lima, and L. G. Ferreira, J. Phys. B **40**, 3015 (2007).

[13] M. A. Khakoo, C. E. Beckmann, S. Trajmar, and G. Csanak, J. Phys. B **27**, 3159 (1994).

[14] J. H. Brunt, G. C. King, and F. H. Read, J. Phys. B **10**, 1289 (1977).

[15] M. A. Khakoo, H. Silva, J. Muse, M. C. A. Lopes, C. Winstead, and V. McKoy, Phys. Rev. A **78**, 052710 (2008).

[16] M. Hughes, K. E. James, Jr., J. G. Childers, and M. A. Khakoo, Meas. Sci. Technol. **14**, 841 (1994).

[17] M. A. Khakoo, K. Keane, C. Campbell, N. Guzman, and K. Hazlett, J. Phys. B **40**, 3601 (2007).

[18] *Handbook of Chemistry and Physics*, 64th ed. (CRC Press, Boca Raton, 1983), p. E-59.

[19] K. Takatsuka and V. McKoy, Phys. Rev. A **24**, 2473 (1981); **30**, 1734 (1984).

[20] C. Winstead and V. McKoy, Comput. Phys. Commun. **128**, 386 (2000).

[21] M. W. Schmidt, K. K. Baldridge, J. A. Boatz, S. T. Elbert, M. S. Gordon, J. H. Jensen, S. Koseki, N. Matsunaga, K. A. Nguyen, S. J. Su, T. L. Windus, M. Dupuis, and J. A. Montgomery, J. Comput. Chem. **14**, 1347 (1993).

[22] B. M. Bode and M. S. Gordon, J. Mol. Graphics Mod. **16**, 133 (1998).

[23] E. Hirota, J. Phys. Chem. **83**, 1457 (1979).

[24] C. W. Bauschlicher, J. Chem. Phys. **72**, 880 (1980).

[25] [http://cccbdb.nist.gov/default.htm].